JOC The Journal of Organic Chemistry

Article

pubs.acs.org/joc

Absolute Asymmetric Photocyclization of Triisopropylbenzophenone Derivatives in Crystals and Their Morphological Changes

Hideko Koshima,*[,†] Michitaro Fukano,[†] Naoko Ojima,[†] Kohei Johmoto,[‡] Hidehiro Uekusa,[‡] and Motoo Shiro[§]

[†]Department of Materials Science and Biotechnology, Graduate School of Science and Engineering, Ehime University, Matsuyama, Ehime 790-8577, Japan

[‡]Department of Chemistry and Materials Science, Tokyo Institute of Technology, 2 Ookayama, Meguro-ku, Tokyo 152-8551, Japan

[§]Rigaku Corporation, 3-9-12 Matsubara, Akishima, Tokyo 196-8666, Japan

Supporting Information

ABSTRACT: Although 4-(2,4,6-triisopropylbenzoyl)benzylbenzamide is an achiral molecule, chiral crystals can form through spontaneous crystallization in a methanol solution. In the *M* crystal, twofold helical hydrogen-bond chains form in a counterclockwise direction among the molecules along the *a* axis to generate crystal chirality. The solid-state circular dichroism spectra of the two enantiomorphous crystals as Nujol mulls show a good mirror-image relationship. UV irradiation of the *M* crystal at >290 nm caused highly enantioselective Norrish type II photocyclization to yield the (*R*)-cyclobutenol with 94% ee in 100% yield as the sole product, resulting in successful absolute asymmetric synthesis. In contrast, the (*S*)-cyclobutenol was obtained from the *P* crystal with 95% ee in 100% yield. The high enantiodifferentiation in the crystalline-state photocyclization is attributed to the shorter distance between the carbonyl oxygen atom and one of the methine γ-hydrogen atoms of the two *o*-isopropyl groups as well as the smooth transformation with minimum molecular motion because of the similar shapes of the reactant and product molecules. UV irradiation of the platelike crystals resulted in a crack in the direction perpendicular to the long axis (the *a* axis of the unit cell), likely because the hydrogen-bond chains were broken during the photocyclization.

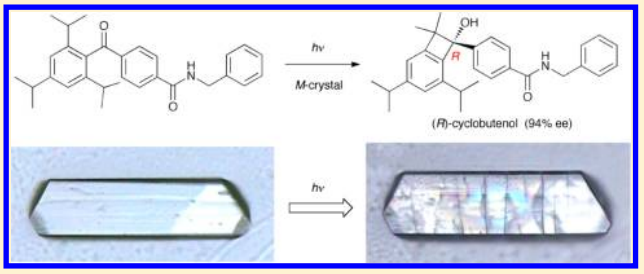

INTRODUCTION

Asymmetric synthesis usually requires an external chiral source, such as a chiral catalyst. In contrast, absolute asymmetric synthesis using chiral crystals that are spontaneously formed from achiral molecules does not require an external chiral source. Since the first report of the absolute asymmetric [2 + 2] photodimerization of butadiene derivatives in mixed crystals in 1973,[1] more than 20 successful examples have been published.[2−6] We also performed the absolute asymmetric photodecarboxylative condensation of acridine with diphenylacetic acid in chiral cocrystals[7] and the absolute asymmetric photocyclization of isopropylbenzophenone in chiral salt crystals.[8] It is known that achiral molecules spontaneously form chiral crystals at 8% statistical probability.[9] However, chiral crystallization of achiral molecules cannot be predicted presently, making it difficult to perform absolute asymmetric syntheses. Nevertheless, we prepared a number of chiral cocrystals composed of two different achiral molecules using a trial-and-error approach.[10−12] Consequently, we realized that chiral crystals could be found in higher probability by learning and using useful information obtained from the molecular arrangements of both chiral and achiral crystals of analogous compounds.

We recently achieved diastereospecific photocyclization in the chiral crystal of an isopropylbenzophenone derivative with an (*S*)-phenylethylamide group.[13] Our success led us to construct chiral crystals of isopropylbenzophenone derivatives substituted with an achiral benzylamide group to identify a novel chiral crystal. Here we report the highly enantioselective photocyclization of 4-(2,4,6-triisopropylbenzoyl)benzylbenzamide (**1**) in chiral crystals and the morphological changes of the single crystals during the photoreaction.

RESULTS AND DISCUSSION

Preparation of Chiral Crystals. Three achiral 2,4,6-triisopropylbenzophenone derivatives with benzylamide groups at the *para*, *meta*, and *ortho* positions (**1**−**3**, respectively) were synthesized and recrystallized from methanol solutions to yield single crystals. X-ray crystallographic analyses of **1**−**3** were performed. They showed that the crystal of **1** was chiral and belonged to an orthorhombic system with space group $P2_12_12_1$ (Table 1). In contrast, the crystals of **2** and **3** revealed an achiral nature with orthorhombic systems showing space groups

Received: January 29, 2014
Published: March 16, 2014

   dx.doi.org/10.1021/jo5000913 | J. Org. Chem. 2014, 79, 3088−3093

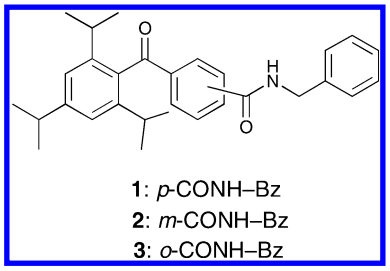

Pna/2_1 and *Pbcn*, respectively. The probability of chiral crystallization of achiral molecules **1**−**3** was 33%, considerably higher than the 8% statistical probability.[9]

The two enantiomeric crystals of **1** were obtained by evaporating the methanol solution and were discriminated using solid-state circular dichroism (CD) spectra as Nujol mulls, which showed a good mirror-image relationship (Figure 1). The absolute structure of **1** was determined using a half piece of the single crystal to be in the *M* form with a high degree of certainty on the basis of the Flack parameter, χ = 0.01(24), in X-ray crystallographic analyses at 93 K.[14] The crystal maintained the same space group, $P2_12_12_1$, but the unit cell size decreased slightly compared with that at 296 K (Table 1). Another half piece of the *M*-**1** single crystal gave the CD curve labeled M in Figure 1; the absolute structure of **1** could be related to the CD spectrum.

Figure 2a shows the ORTEP drawing of molecule **1** in the *M*-**1** crystal at 296 K. The 4-isopropylphenyl group of 2,4,6-triisopropylbenzophenone (blue color) and the phenyl ring of the benzyl group (green color) were disordered with 0.234 and 0.329 occupancy, respectively. Molecule **1** showed a torsional conformation: the dihedral angle between the triisopropylbenzene plane and the phenyl plane of triisopropylbenzophenone was 85.71° (almost perpendicular), and the dihedral angles between the phenyl plane of triisopropylbenzophenone and the disordered phenyl plane of the benzyl group were 65.29° (0.671 occupancy) and 60.13° (0.329 occupancy). In the *M*-**1** crystal, twofold helical hydrogen-bond chains formed in a counterclockwise (minus, *M*) direction among the benzophenone carbonyl groups and the amide groups through C═O···H−N (2.28 Å) interactions along the *a* axis (Figure 2b,c). In contrast, clockwise (plus, *P*) helical chains alone are arranged in the *P* crystal. The helical chains are alternately arranged in opposite directions with a half translation along the *c* axis, which induces the crystal chirality.

Solid-State Photoreaction. Both enantiomorphous crystals of **1** for the solid-state photoreaction were prepared by seeding on a large scale and differentiated on the basis of their

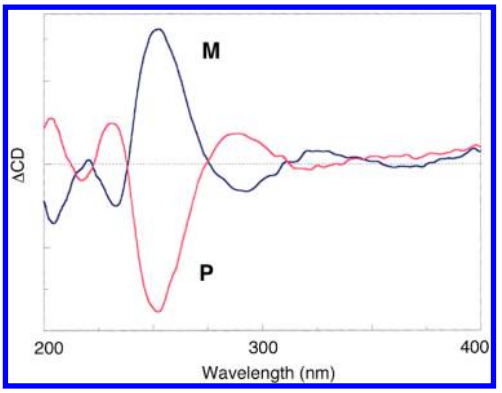

Figure 1. Solid-state CD spectra of the enantiomorphous *M*-**1** and *P*-**1** crystals as Nujol mulls.

solid-state CD spectra (Figure 1). UV irradiation of the pulverized crystals of *M*-**1** with a high-pressure mercury lamp through Pyrex (>290 nm) under argon at 15 °C for 24 h caused highly enantioselective photocyclization to yield chiral cyclobutenol **4** as the sole product in 100% chemical yield (Scheme 1). The enantiomeric excess was determined to be 94% ee on the basis of high-performance liquid chromatography (HPLC) using a chiral column.

The absolute configuration of product **4** was determined as follows (Scheme 2). We previously reported that 4-(2,4,6-triisopropylbenzoyl)benzoic acid (**5**) undergoes enantioselective photocyclization in the three-component cocrystal with L-prolinol and water via a single-crystal-to-single-crystal transformation to yield the *R*-form cyclobutenol (*R*)-**6** with 30% ee as the sole product.[15] At this time, we performed the same photoreaction of the cocrystal and obtained (*R*)-**6** with 15% ee. Cyclobutenol (*R*)-**6** was then transformed into the benzylamide derivative (*R*)-**4** through a reaction with benzylamine in the presence of BOP and triethylamine. Chiral HPLC analysis revealed the first peak (retention time, 11.6 min) and second peak (retention time, 24.3 min) corresponding to (*S*)-**4** and (*R*)-**4**, respectively, and the enantiomeric excess of (*R*)-**4** was determined to be 12% ee (Scheme 2). Consequently, the reaction of *M*-**1** crystals yielded the *R*-form cyclobutenol (*R*)-**4** with 94% ee. UV irradiation of the opposite-handed *P*-**1** crystals yielded (*S*)-**4** alone in 100% chemical yield with 95% ee. In contrast, solution photolysis of **1** in acetonitrile yielded a racemic mixture of (*R*)- and (*S*)-**4** in 65% chemical yield.

Figure 3 shows the possible reaction paths in the *M*-**1** crystal. Photoirradiation of the *M*-**1** crystal at >290 nm with a high-pressure mercury lamp through Pyrex causes n,π^* excitation of

Table 1. Selected Crystal Data

	1	*M*-**1**	**2**	**3**	*rac*-**4**
T (K)	296	93	296	296	296
crystal system	orthorhombic	orthorhombic	orthorhombic	orthorhombic	monoclinic
space group	$P2_12_12_1$ (No. 19)	$P2_12_12_1$ (No. 19)	*Pna*/2_1 (No. 33)	*Pbcn* (No. 60)	*C*2/*c* (No. 15)
a (Å)	9.340(3)	9.30070(17)	26.203(3)	34.511(3)	34.467(4)
b (Å)	11.0137(10)	10.82862(17)	8.9809(9)	8.6859(8)	16.0663(18)
c (Å)	25.4582(11)	24.9809(7)	11.0665(11)	18.3438(17)	9.5149(10)
β (deg)	90.0	90.0	90.0	90.0	93.017(7)
V (Å^3)	2618.8(9)	2515.91(9)	2604.2(5)	5498.7(9)	5261.6(11)
Z	4	4	4	8	8
D (g cm^{-3})	1.120	1.166	1.126	1.067	1.115
Flack parameter	–	0.01(24)	–	–	–

dx.doi.org/10.1021/jo5000913 | *J. Org. Chem.* 2014, 79, 3088−3093

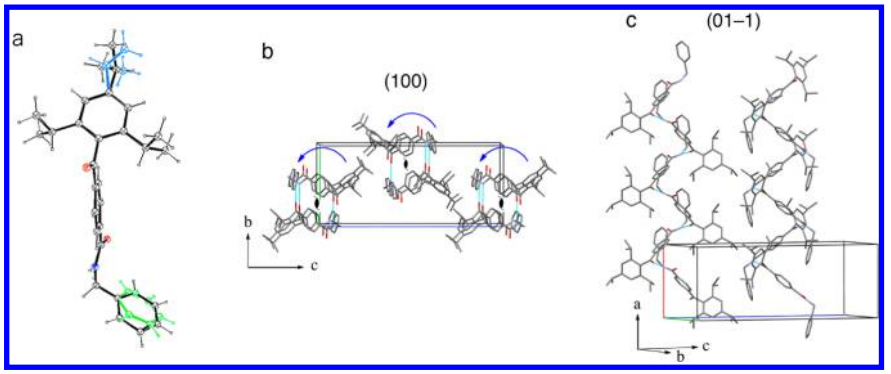

Figure 2. (a) ORTEP drawing of molecule **1** in the *M*-**1** crystal at 296 K; the thermal ellipsoids are plotted at the 25% probability level. The 4-isopropyl group (blue color) and the phenyl ring (green color) are disordered with 0.234 and 0.329 occupancy, respectively. (b, c) Molecular arrangements on (b) the (100) face and (c) the (01$\bar{1}$) face. Counterclockwise twofold helical hydrogen-bond chains (blue dotted lines) form along the *a* axis. The hydrogen atoms in (b) and (c) have been omitted for clarity, and the disordered 4-isopropyl group and the phenyl ring have also been omitted.

Scheme 1. Solid-State Photoreaction of the Enantiomorphous *M*-1 and *P*-1 Crystals

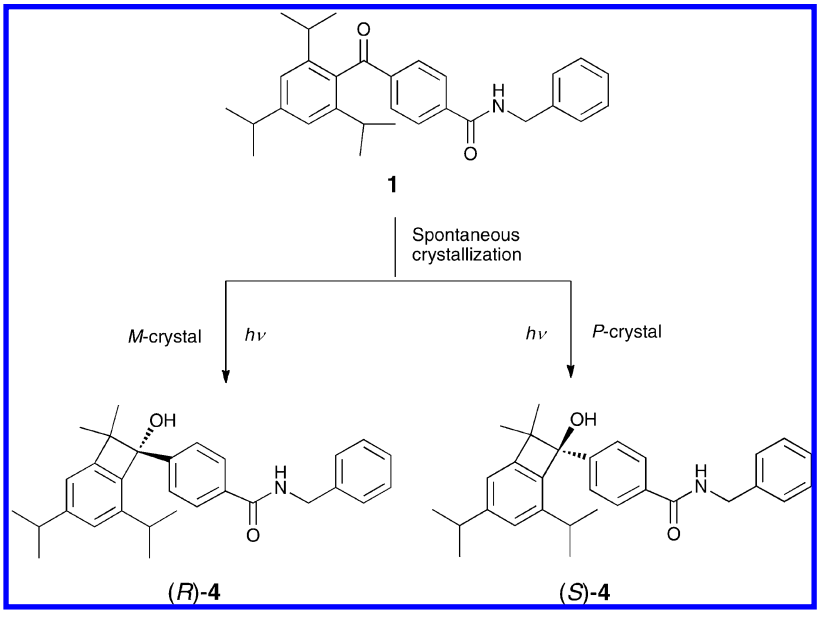

Scheme 2. Enantioselective Photocyclization through Single-Crystal-to-Single-Crystal Transformation and Determination of the Absolute Configuration of Product 4

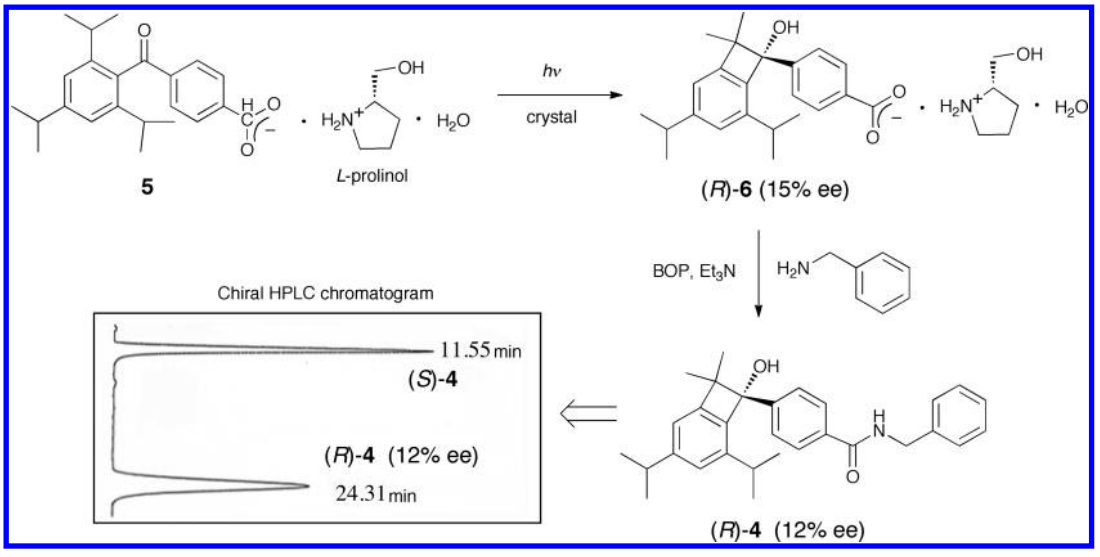

dx.doi.org/10.1021/jo5000913 | J. Org. Chem. 2014, 79, 3088−3093

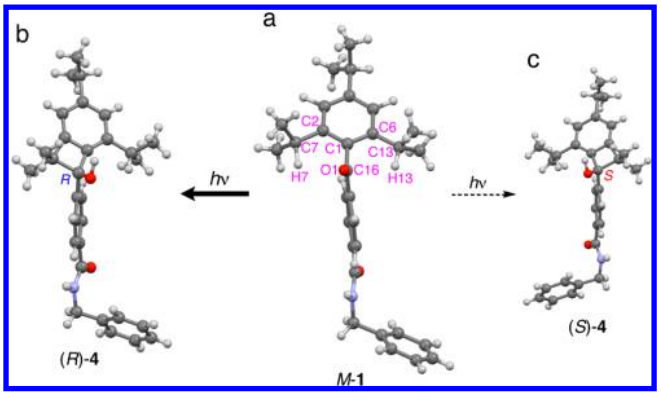

Figure 3. Possible reaction paths for enantioselective photocyclization: (a) reactant molecule **1** in the *M*-**1** crystal; (b, c) product molecules (b) (*R*)-**4** and (c) (*S*)-**4** coexisting in the racemic crystal *rac*-**4** obtained by solution photolysis of **1**. The disordered isopropyl and phenyl groups in the molecules of **1**, (*R*)-**4**, and (*S*)-**4** have been omitted for clarity.

the carbonyl oxygen atom (O1) of molecule **1** (Figure 3a). The excited O1 atom can release the methine hydrogen atoms of two *o*-isopropyl groups (H7 and H13) to produce the (*R*)- and (*S*)-ketyl radicals (·C16), respectively, and the corresponding methine radicals (·C7 and ·C13). The radicals approach each other and finally couple to produce (*R*)- and (*S*)-cyclobutenol [i.e., the enantiomeric products (*R*)-**4** and (*S*)-**4**, respectively]. However, (*R*)-**4** was obtained with high enantioselectivity (94% ee) through the crystalline-state photocyclization. Hence, the geometrical parameters for the two possible γ-hydrogen atom abstractions were compared: the O1−C16−C1−C2 and O1−C16−C1−C6 torsion angles are −80.92° and 100.05°, respectively, and the O1 atom is tilted toward the C7 by 9.6°. Thus, the O1···H7 distance (2.65 Å) is shorter than the O1···H13 distance (2.99 Å) by 0.34 Å, leading to abstraction of H7 with higher priority than H13, yielding (*R*)-cyclobutenol (*R*)-**4** with higher enantioselectivity than (*S*)-**4**.[16] However, it is not clear why very high enantiodifferentiation of (*R*)-**4** (94% ee) results from the shorter distance of hydrogen abstraction.

As a matter of course, the *o*-isopropyl groups and the carbonyl group of the reactant *M*-**1** move upon the occurrence of hydrogen abstraction by the excited carbonyl oxygen, and thus, a larger surrounding space is advantageous. The surrounding area, a cavity, is defined as a space limited by a concave surface of the spheres of inter- and intramolecular atoms in the neighborhood.[17] The cavity size of 3.8 Å required to yield (*R*)-**4** is larger than that to yield (*S*)-**4** (2.7 Å), supporting the preferential enantioselective formation of (*R*)-**4** from the *M*-**1** crystal (Figure 4).

Solid-state reactions generally proceed with minimum molecular motion in the crystal lattice because the molecules are arranged at close positions in three-dimensional regularity and thus the motion is very restricted. In contrast, the molecules are arranged with the most stable conformation in the crystal from solution. Thus, the molecular conformation of a product in a solid-state reaction often differs from that of a product crystallized from solution. Nevertheless, it is meaningful that the reaction path is discussed on the basis of the most stable conformation of the molecules in the product crystal. At this time, enantiomorphous crystals of (*R*)-**4** did not form by recrystallization from solution of the photoproducts from the solid-state photoreaction of the *M*-**1** crystals. However, racemic crystals of *rac*-**4** were obtained by

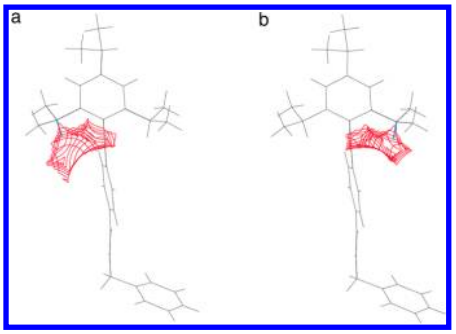

Figure 4. Drawings of cavities for the *o*-isopropyl groups and the carbonyl group in the *M*-**1** crystal to produce the enantiomers (a) (*R*)-**4** and (b) (*S*)-**4**.

recrystallization from 2-propanol solution of the racemic mixture of (*R*)-**4** and (*S*)-**4** obtained from the solution photolysis of **1**. Crystallographic analysis of *rac*-**4** was successful (Table 1). The reaction path in the *M*-**1** crystal is discussed on the basis of the most stable conformation of (*R*)- and (*S*)-**4** molecules in the racemic *rac*-**4** crystal.

The molecular conformation of (*R*)-**4** in the *rac*-**4** crystal (Figure 3b) is similar to that of reactant **1** in the *M*-**1** crystal (Figure 3a). This suggests that the transformation from molecule **1** to (*R*)-**4** should proceed smoothly upon UV irradiation because of the minimum motion within the helical chains in the *M*-**1** crystal. In contrast, the molecular conformation of (*S*)-**4** in the *rac*-**4** crystal (Figure 3c) differs significantly from that of molecule **1** in the *M*-**1** crystal because the phenyl ring of the benzylamide group is twisted to the opposite side. Hence, a large motion would be required to turn the phenyl ring to the opposite side and produce the (*S*)-**4** molecule in the *M*-**1** crystal. However, it would be difficult to achieve such a large molecular motion within the restricted crystal lattice. This may also explain why (*S*)-**4** is rarely produced but (*R*)-**4** shows very high enantioselectivity (94% ee).

We observed morphological changes of the microcrystals of **1** during photocyclization using a CCD microscope. Figure 5a shows a piece of the platelike microcrystal before irradiation. The top surface is the $(01\bar{1})$ face, and the long axis is the *a* axis. UV irradiation of the microcrystal for 1 h resulted in a crack in the direction perpendicular to the long axis (Figure 5b). The

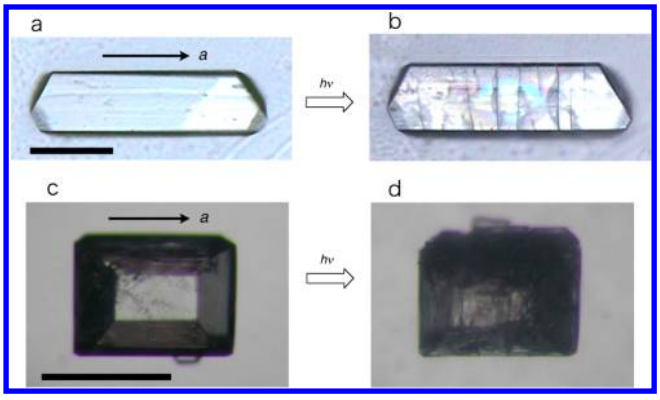

Figure 5. (a, b) Morphological changes of a microcrystal of **1** (a) before and (b) after UV irradiation for 1 h. The scale bar is 100 μm. (c, d) Morphological changes of a bulk crystal of **1** (c) before and (d) after UV irradiation for 15 h. The scale bar is 1.0 mm.

dx.doi.org/10.1021/jo5000913 | J. Org. Chem. 2014, 79, 3088−3093

bulk single crystal of **1** also cracked in the direction perpendicular to the long axis after UV irradiation for 15 h (Figure 5c,d). In the reactant crystal of **1**, twofold helical hydrogen-bond chains form among the benzophenone carbonyl groups and the amide groups through C═O···H−N interactions along the *a* axis (Figure 2b,c), which is the long axis of the platelike crystal (Figure 5). When the benzophenone C═O group of molecule **1** is transformed into the cyclobutenol O−H group of product molecule **4** by the Norrish type II hydrogen abstraction followed by cyclization upon UV irradiation, the hydrogen-bond chains along the *a* axis inevitably break.

The reaction process could be traced by the changes in the Fourier-transform infrared (FT-IR) spectrum. The 1640 cm^{-1} band of the stretching vibration of the benzophenone C═O group in molecule **1** decreased as a result of the change to the cyclobutenol O−H group in product molecule **4** with increasing UV irradiation time (Figure 6a). The 1247 cm^{-1} band corresponding to interactions among the C═O stretching, N−H bending, and C−N stretching of the amide in reactant molecule **1** also decreased upon UV irradiation. The amide group is not involved in the photocylization reaction, but the C═O···H−N hydrogen bond chains along the *a* axis break as a result of the change from the benzophenone C═O group to the cyclobutenol O−H group as the reaction proceeds. The 1247 cm^{-1} band is susceptible to the change in the crystalline environment due to the reaction, and thus, its strength decreases with increasing UV irradiation time. The conversion of the photocyclization, based on the intensity changes in the absorption at 1247 cm^{-1}, showed an almost linear relationship with irradiation time (Figure 6b). With UV irradiation for 1 h, around 80% of the hydrogen-bond chains along the long axis of the crystals were estimated to be broken. This may explain why the crystals cracked in the direction perpendicular to the long axis during photocyclization.

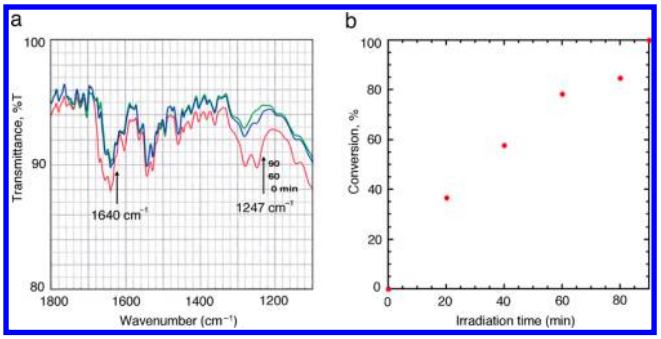

Figure 6. (a) Changes in the IR spectra and (b) conversion of the photocyclization of **1** in the microcrystals under UV irradiation.

CONCLUSIONS

Absolute asymmetric photocyclization of 4-(2,4,6-triisopropylbenzoyl)benzylbenzamide was achieved in the crystalline state. Irradiation of the *M* crystal caused highly enantioselective Norrish type II photocyclization to yield the (*R*)-cyclobutenol with 94% ee in 100% yield as the sole product. The high enantiodifferentiation in the solid-state photocyclization is attributed to the shorter distance between the carbonyl oxygen atom and one of the methine γ-hydrogen atoms of the two *o*-isopropyl groups as well as the smooth transformation with minimum molecular motion as a result of the very similar molecular shapes of the reactant and the product. The platelike single crystals cracked upon UV irradiation in the direction perpendicular to the long axis, likely because of breaking of the hydrogen-bond chains in the reactant crystals during photocyclization.

EXPERIMENTAL SECTION

General Information. All melting points are uncorrected. ^{1}H NMR and ^{13}C NMR spectra were recorded using a 400 MHz NMR instrument. Chemical shifts are reported in parts per million relative to tetramethylsilane. IR spectra were recorded on an FT-IR instrument, and samples were analyzed as films with KBr. The solvents were of analytical grade.

4-(2,4,6-Triisopropylbenzoyl)benzylbenzamide (1). 2,4,6-Triisopropyl-4′-carboxybenzophenone (0.401 g, 1.14 mmol) and benzylamine (0.379 g, 3.54 mmol) were dissolved in chloroform (10 mL) and THF (10 mL), and triethylamine (4.0 mL, 28 mmol) and BOP (1.073 g, 2.43 mmol) were added. The solution was stirred at room temperature for 15 h, and the solvent was evaporated under vacuum. The crude product was purified via silica gel column chromatography (hexane/ethyl acetate, 10:1) to afford **1** (0.333 g, 0.75 mmol, 66% yield) as a white powder. Mp 206.3−207.2 °C; ^{1}H NMR (400 MHz, $CDCl_3$) δ 7.90−7.83 (m, 4H), 7.37−7.31 (m, 5H), 7.06 (s, 2H), 6.41 (bs, 1H), 4.66 (d, J = 5.6 Hz, 2H), 2.94 (septet, J = 6.8 Hz, 1H), 2.56 (septet, J = 6.8 Hz, 2H), 1.30 (d, J = 6.8 Hz, 6H), 1.16 (d, J = 6.8 Hz, 6H), 1.04 (d, J = 6.8 Hz, 6H); ^{13}C NMR (100 MHz, $CDCl_3$) δ 200.5, 166.5, 150.1, 145.0, 140.3, 138.6, 137.8, 134.5, 129.7, 128.9, 128.0, 127.8, 127.3, 121.1, 96.1, 44.3, 34.4, 31.1, 24.9, 24.0, 23.4; IR (cm^{-1}) 3426, 3033, 2960, 2929, 2869, 1658, 1604, 1531, 1494, 1458, 1385, 1361, 1319, 1281, 1139, 948, 922, 876, 732. Anal. Calcd for $C_{30}H_{35}NO_2$: C, 81.59; H, 7.99; N, 3.17. Found: C, 81.38; H, 7.73; N, 3.14.

3-(2,4,6-Triisopropylbenzoyl)benzylbenzamide (2). 2,4,6-Triisopropyl-3′-carboxybenzophenone (0.400 g, 1.13 mmol) and benzylamine (0.368 g, 3.43 mmol) were dissolved in chloroform (10 mL) and THF (10 mL), and triethylamine (4.0 mL, 28 mmol) and BOP (1.073 g, 2.43 mmol) were added. The solution was stirred at room temperature for 15 h, and the solvent was evaporated under vacuum. The crude product was purified via silica gel column chromatography (hexane:/ethyl acetate, 10:1) to afford **2** (0.400 g, 0.91 mmol, 80% yield) as a white powder. Mp 147.5−149.8 °C; ^{1}H NMR (400 MHz, $CDCl_3$) δ 8.36 (s, 1H), 8.11 (d, J = 7.8 Hz, 1H), 7.78 (d, J = 7.8 Hz, 1H), 7.51 (t, J = 7.8 Hz, 1H), 7.31−7.38 (m, 5H), 7.06 (s, 2H), 6.52 (bs, 1H), 4.66 (d, J = 5.6 Hz, 2H), 2.93 (septet, J = 6.8 Hz, 1H), 2.56 (septet, J = 6.8 Hz, 2H), 1.29 (d, J = 6.8 Hz, 6H), 1.16 (d, J = 6.8 Hz, 6H), 1.05 (d, J = 6.8 Hz, 6H); ^{13}C NMR (100 MHz, $CDCl_3$) δ 200.6, 166.3, 150.1, 145.0, 138.3, 137.8, 135.1, 134.3, 133.3, 132.6, 129.1, 128.9, 128.0, 127.8, 126.0, 121.2, 96.1, 44.3, 34.4, 31.2, 24.9, 24.0, 23.4; IR (cm^{-1}) 3421, 2958, 1678, 1658, 1599, 1534, 1460, 1426, 1385, 1362, 1322, 1249, 1185, 1106, 954, 875, 731. Anal. Calcd for $C_{30}H_{35}NO_2$: C, 81.59; H, 7.99; N, 3.17. Found: C, 81.46; H, 7.74; N, 3.08.

2-(2,4,6-Triisopropylbenzoyl)benzylbenzamide (3). 2,4,6-Triisopropyl-2′-carboxybenzophenone (0.400 g, 1.13 mmol) and benzylamine (0.365 g, 3.43 mmol) were dissolved in chloroform (10 mL) and THF (10 mL), and triethylamine (4.0 mL, 28 mmol) and BOP (1.072 g, 2.40 mmol) were added. The solution was stirred at room temperature for 15 h, and the solvent was evaporated under vacuum. The crude product was purified via silica gel column chromatography (hexane/ethyl acetate, 10:1) to afford **3** (0.293 g, 0.91 mmol, 59% yield) as a white powder. Mp 116.2−118.0 °C; ^{1}H NMR (400 MHz, $CDCl_3$) δ 7.56−7.52 (m, 2H), 7.48 (d, J = 7.2 Hz, 2H), 7.41−7.30 (m, 5H), 7.06 (s, 2H), 6.13 (bs, 1H), 4.74 (d, J = 5.6 Hz, 2H), 2.93 (septet, J = 6.8 Hz, 1H), 2.76 (septet, J = 6.8 Hz, 2H), 1.29 (d, J = 6.8 Hz, 6H), 1.10 (bs, 12H); ^{13}C NMR (100 MHz, $CDCl_3$) δ 200.4, 170.0, 150.1, 145.5, 138.2, 137.5, 136.7, 134.9, 132.7, 132.0, 129.3, 128.7, 128.2, 127.5, 121.1, 96.1, 44.4, 34.4, 30.9, 24.0; IR (cm^{-1}) 3248, 3065, 2961, 2868, 1678, 1635, 1601, 1553, 1459, 1383, 1362, 1291,

dx.doi.org/10.1021/jo5000913 | J. Org. Chem. 2014, 79, 3088−3093

1250, 1157, 947, 919, 879, 746. Anal. Calcd for $C_{30}H_{35}NO_2$: C, 81.59; H, 7.99; N, 3.17. Found: C, 81.70; H, 7.69; N, 3.18.

Photoreaction of the *M*-1 and *P*-1 Crystals. Pulverized *M*-**1** crystals (0.200 g, 0.45 mmol) were placed between two Pyrex plates and irradiated with a 400 W high-pressure mercury lamp under argon at 15 °C for 24 h to yield cyclobutenol **4** (0.200 g, 0.45 mmol, 100% yield) as the sole product. Mp 158.2−159.3 °C; ^{1}H NMR (400 MHz, $CDCl_3$) δ 7.73 (d, J = 8.4 Hz, 2H), 7.37−7.30 (m, 5H), 7.06 (s, 2H), 6.89 (s, 1H), 6.36 (bs, 1H), 4.66 (d, J = 5.6 Hz, 2H), 2.92 (septet, J = 6.8 Hz, 1H), 2.83 (septet, J = 6.8 Hz, 1H), 1.45 (s, 3H), 1.28 (d, J = 6.8 Hz, 6H), 1.19 (d, J = 6.8 Hz, 3H), 1.15 (d, J = 6.8 Hz, 3H), 0.80 (s, 3H); ^{13}C NMR (100 MHz, $CDCl_3$) δ 167.3, 152.8, 151.7, 146.5, 145.1, 139.5, 138.2, 133.0, 128.8, 128.0, 127.6, 127.0, 126.4, 124.2, 116.2, 96.1, 85.6, 54.8, 44.1, 35.0, 30.5, 24.6, 24.4, 24.3, 24.1, 22.8; IR (cm^{-1}) 3423, 2959, 1651, 1528, 1496, 1458, 1362, 1283, 1194, 1060, 917, 872, 751. Anal. Calcd for $C_{30}H_{35}NO_2$: C, 81.59; H, 7.99; N, 3.17. Found: C, 81.70; H, 8.21; N, 3.12. The absolute configuration of the product **4** was confirmed to be *R* (see the details of the determination method in the Results and Discussion). The enantiomeric excess was determined to be 94% ee by HPLC using a chiral column (Daicel, Chiralpak AD) and hexane/2-propanol with monitoring at 210 nm.

Solution Photolysis of 1. A solution of **1** (2.21 g, 5.00 mmol) in acetonitrile (100 mL) was internally irradiated with a 100 W high-pressure mercury lamp at room temperature for 55 h under bubbling of argon. The solvent was evaporated from the irradiated solution, and the residue was submitted to silica gel column chromatography (hexane/ethyl acetate, 10:1) to yield racemic **4** (1.44 g, 3.25 mmol, 65% yield) as the sole product and remaining starting material **1** (0.751 g, 1.70 mmol, 66% conversion). Data for *rac*-**4**: mp 171.2−172.3 °C (from hexane and 2-propanol); ^{1}H NMR (400 MHz, $CDCl_3$) δ 7.73 (d, J = 8.4 Hz, 2H), 7.37−7.30 (m, 5H), 7.06 (s, 2H), 6.89 (s, 1H), 6.36 (bs, 1H), 4.66 (d, J = 5.6 Hz, 2H), 2.92 (septet, J = 6.8 Hz, 1H), 2.83 (septet, J = 6.8 Hz, 1H), 1.45 (s, 3H), 1.28 (d, J = 6.8 Hz, 6H), 1.19 (d, J = 6.8 Hz, 3H), 1.15 (d, J = 6.8 Hz, 3H), 0.80 (s, 3H); ^{13}C NMR (100 MHz, $CDCl_3$) δ 167.3, 152.8, 151.7, 146.4, 145.1, 139.4, 138.2, 133.0, 128.8, 128.0, 127.6, 127.0, 126.4, 124.2, 116.2, 96.1, 85.6, 54.8, 44.1, 35.0, 30.5, 24.6, 24.4, 24.2, 24.1, 22.8; IR (cm^{-1}) 3423, 2959, 1651, 1528, 1496, 1458, 1362, 1283, 1194, 1060, 917, 872, 751. Anal. Calcd for $C_{30}H_{35}NO_2$: C, 81.59; H, 7.99; N, 3.17. Found: C, 81.75; H, 8.19; N, 3.10.

X-ray Crystallograhic Analysis. X-ray crystallographic analysis was performed on an X-ray diffractometer using a two-dimensional imaging plate area detector (Rigaku RAXIS-RAPID) with Cu Kα radiation (λ = 1.54187 Å). All of the crystallographic calculations were performed using crystallographic software (Rigaku CrystalStructure 3.8 and 4.0).[18] Structures were determined using direct methods and expanded using Fourier techniques. The non-hydrogen atoms were refined anisotropically, and the hydrogen atoms were not refined. Hydrogen atoms attached to carbon atoms were located in the calculated positions. The absolute structure of **1** was determined from the Flack parameter.[14] The crystal data are summarized in Table 1. The data in CIF format have been deposited at the Cambridge Crystallographic Data Centre with deposition numbers CCDC 973507 (**1**), CCDC 973508 (*M*-**1**), CCDC 973509 (**2**), CCDC 973510 (**3**), and CCDC 973511 (*rac*-**4**).

■ ASSOCIATED CONTENT

Ⓢ Supporting Information

^{1}H and ^{13}C NMR spectra for **1**−**4** and labeled ORTEP diagrams and CIFs for **1**, *M*-**1**, **2**, **3**, and *rac*-**4**. This material is available free of charge via the Internet at http://pubs.acs.org.

■ AUTHOR INFORMATION

Corresponding Author

*Tel: +81-89-927-8523. Fax: +81-89-927-8523. E-mail: koshima.hideko.mk@ehime-u.ac.jp.

Notes

The authors declare no competing financial interest.

■ ACKNOWLEDGMENTS

This work was supported by Grants-in-Aid for Scientific Research (B) (22350063) and Challenging Exploratory Research (23655129) from the Japan Society for the Promotion of Science.

■ REFERENCES

(1) Elgavi, A.; Green, B. S.; Schmidt, G. M. J. *J. Am. Chem. Soc.* **1973**, *95*, 2058−2059.
(2) Green, B. S.; Lahav, M.; Ravinovich, D. *Acc. Chem. Res.* **1979**, *12*, 191−197.
(3) Feringa, B. L.; van Delden, R. A. *Angew. Chem., Int. Ed.* **1999**, *38*, 3418−3438.
(4) Koshima, H. In *Organic Solid-State Reactions*; Toda, F., Ed.; Kluwer Academic Publishers: Dordrecht, The Netherlands, 2002; pp 189−268.
(5) Koshima, H. In *Chiral Photochemistry*; Inoue, Y., Ramamurthy, V., Eds.; Marcel Dekker: New York, 2004; pp 485−531.
(6) Sakamoto, M. *J. Photochem. Photobiol., C* **2006**, *7*, 183−196.
(7) Koshima, H.; Ding, K.; Chisaka, Y.; Matsuura, T. *J. Am. Chem. Soc.* **1996**, *118*, 12059−12065.
(8) Koshima, H.; Kawanishi, H.; Nagano, M.; Yu, H.; Shiro, M.; Hosoya, T.; Uekusa, H.; Ohashi, Y. *J. Org. Chem.* **2005**, *70*, 4490−4497.
(9) Matsuura, T.; Koshima, H. *J. Photochem. Photobiol., C* **2005**, *6*, 7−24.
(10) (a) Koshima, H.; Hayashi, E.; Matsuura, T.; Tanaka, K.; Toda, F.; Kato, M.; Kiguchi, M. *Tetrahedron Lett.* **1997**, *38*, 5009−5012. (b) Koshima, H.; Nakagawa, T.; Matsuura, T.; Miyamoto, H.; Toda, F. *J. Org. Chem.* **1997**, *62*, 6322−6325. (c) Koshima, H.; Hayashi, E.; Matsuura, T. *Supramol. Chem.* **1999**, *11*, 57−66. (d) Koshima, H.; Nakata, A.; Nagano, M.; Yu, H. *Heterocycles* **2003**, *60*, 2251−2258.
(11) (a) Koshima, H.; Khan, S. I.; Garcia-Garibay, M. A. *Tetrahedron: Asymmetry* **1998**, *9*, 1851−1854. (b) Koshima, H.; Honke, S. *J. Org. Chem.* **1999**, *64*, 790−793. (c) Koshima, H.; Honke, S.; Fujita, J. *J. Org. Chem.* **1999**, *64*, 3916−3921.
(12) (a) Koshima, H.; Hamada, M.; Yagi, I.; Uosaki, K. *Cryst. Growth Des.* **2001**, *1*, 467−471. (b) Koshima, H.; Miyamoto, H.; Yagi, I.; Uosaki, K. *Cryst. Growth Des.* **2004**, *4*, 807−811.
(13) (a) Koshima, H.; Fukano, M.; Uekusa, H. *J. Org. Chem.* **2007**, *72*, 6786−6791. (b) Fujii, K.; Uekusa, H.; Fukano, M.; Koshima, H. *CrystEngComm* **2011**, *13*, 3197−3201.
(14) Flack, H. D. *Acta Crystallogr.* **1983**, *A39*, 876−881.
(15) (a) Koshima, H.; Maeda, A.; Matsuura, T.; Hirotsu, K.; Okada, K.; Mizutani, H.; Ito, Y.; Fu, T. Y.; Scheffer, J. R.; Trotter, J. *Tetrahedron: Asymmetry* **1994**, *5*, 1415−1418. (b) Hirotsu, K.; Okada, K.; Mizutani, H.; Koshima, H.; Matsuura, T. *Mol. Cryst. Liq. Cryst.* **1996**, *277*, 99−106.
(16) Scheffer, J. F. In *Organic Solid State Chemistry*; Desiraju, G. R., Ed.; Elsevier: New York, 1987; pp 1−45.
(17) Ohashi, Y.; Yanagi, K.; Kurihara, T.; Sasada, Y.; Ohgo, Y. *J. Am. Chem. Soc.* **1981**, *103*, 5805−5812.
(18) *CrystalStructure*, versions 3.8 and 4.0; Rigaku Corporation: Tokyo, 2005.